Desalination and Water Treatment
www.deswater.com
doi: 10.1080/19443994.2015.1049555

57 (2016) 12178–12191
June

Taylor & Francis
Taylor & Francis Group

Efficient adsorption of copper ion from aqueous solution by amino-functioned porous eggshell membrane

Jian Hua Chen[a,b,*], Yi Hong Huang[a]

[a]*College of Chemistry and Environmental, Minnan Normal University, Zhangzhou 363000, China, Tel. +86 596 2591445; Fax: +86 596 2520035; email: jhchen73@126.com (J.H. Chen)*
[b]*Fujian Province University Key Laboratory of Modern Analytical Science and Separation Technology, Minnan Normal University, Zhangzhou 363000, China*

Received 20 September 2014; Accepted 1 May 2015

ABSTRACT

A novel porous membrane adsorbent was prepared by grafting of amino groups onto surface of eggshell membrane (Amino-ESM). Adsorption property of the Amino-ESM was investigated by removing Cu(II) ions from aqueous solution. Physicochemical properties of the pristine and the Cu(II)-loaded Amino-ESM were characterized by the FT-IR, SEM-energy dispersive X-ray, and contact angle goniometer methods. Meanwhile, effects of several important parameters, such as the amount of ammonia using for grafting, solution pH, temperature, contact time, and ionic strength, on adsorption behavior were studied by batch experiments. Adsorption capacity of the as-prepared Amino-ESM was about 2.5 times higher than that of the pristine ESM. The adsorption rate was rapid, and the equilibrium adsorption could be achieved within 60 min. Effect of ionic strength on the Amino-ESM adsorption was slight. Adsorption behavior was favorable and endothermic. Moreover, kinetics experiments indicated that the pseudo-first-order model displayed the best correlation with adsorption kinetics data. Besides, the intraparticle diffusion model and Crank model showed that the intraparticle solute diffusion is the rate-controlling step. Finally, adsorption experimental data could be better described by the Freundlich isotherm model. These results suggested that the prepared Amino-ESM could be an efficient adsorbent for removing Cu(II) ions from aqueous solution.

Keywords: Amino-functioned; Eggshell membrane; Cu(II); Adsorption

1. Introduction

Copper is one of the most widespread heavy metal with broad range of applications such as catalysts, fertilizers, stabilizers, and pigments [1–6]. However, the discharge of copper from various industries into the environment has resulted in a number of environmental problems. The heavy metals such as copper, chromium, zinc, and cadmium have become a major issue throughout the world. Although copper is a bio-essential element, for example, the adult daily need for human beings estimated to be 2 mg, ecological impacts may be observed when copper concentration exceeds 0.2 mg/L. Intake of excessive dosage of copper by humans may lead to severe diseases such as mucosal irritation and corrosion, central nervous system irritation followed by depression, and possible

*Corresponding author.

necrotic changes in the liver and kidney [7]. As a result, the permissible limit of copper in drinking water stipulated by the US Environmental Protection Agency (EPA) is 1.3 mg/L [8].

Removal of Cu(II) ions from wastewater by adsorption has been investigated by many researchers [9–12]. The main advantages of the adsorption are the recovery of heavy metals, producing of less volume of sludge, simplicity of design, and the meeting of strict discharge specification. When concentration of heavy metals is less than 100 mg/L, the most suitable and effective method for heavy metal removal has been proven to be adsorption [13]. Owing to the faster rate of the metal ions to be removed can be brought to the internal binding sites in the porous adsorptive membrane adsorbent than that of absorptive beads, investigating into the adsorption property of the porous adsorptive membrane adsorbent is becoming more and more attractive [14,15].

In recent years, more and more attentions have been focused on the use of naturally available low-cost biomaterials for removing heavy metals from wastewater [16–19]. Adsorption of heavy metal from wastewater using biomaterials can reduce total capital cost greatly, as compared with other traditional treatment processes. Meanwhile, using of biomaterials also makes the adsorption process more environmental friendly. Eggshell membrane (ESM), as a byproduct of egg, is a cheap, green and easily available biological material with complex porous structure. It is mainly composed of protein fibers (approximately 95%) and has high surface area, excellent chemical stability, and high density of surface functional groups including amines, amides, hydroxyl, and carboxyl, which made it as a promising adsorbent for wastewater treatment [20]. Every day, a huge amount of eggs were consumed all over the world. However, most of eggshell was simply disposed of for landfill without any pretreatment. Based on the bio-resource recovery and reuse, the utilization of this food processing byproduct has slightly increased in recent years. Yoo et al. [21] utilized calcium carbonate particles from eggshell waste as coating pigments for ink-jet printing paper. Torres et al. [22] studied structure–property relationships of ESM network with the aim to explore the potential applications of ESM in biomedicine. Wei et al. [23] used waste eggshell as a solid catalyst in triglyceride transesterification with a view to determine its viability for use in biodiesel synthesis. Tang et al. [24] used ESM as immobilization platform in sandwich immunoassay. Gergely et al. [25] prepared hydroxyapatite from eggshell. Zhang et al. [26] used ESM-based solid-phase extraction combined with hydride generation atomic fluorescence spectrometry for trace arsenic (V) in environmental water samples. Zheng et al. [27] has prepared gold nanoparticles on ESM and investigated their biosensing application. In a word, as a natural biomaterial, ESM will be found its application in a more wide range.

Therefore, based on the aforementioned considerations, the overall goal of this study was to explore the potential application of the ESM for adsorption removing Cu(II) ions from wastewater. Amino groups have been demonstrated to be an effective functional groups for removing heavy metals because of the presence of chelating ligands of –N: on it [28]. Therefore, we try to improve the adsorption performance of the ESM for Cu(II) ions by grafting amino groups onto its surface. Batch adsorption experiments were carried out to investigate the effects of several important factors, such as amount of ammonia using for grafting, contact time, solution pH, contact time, and initial concentration of Cu(II) ions, on the uptake capacity of Amino-ESM. The adsorption property of the Amino-ESM for Cu(II) ions was analyzed by fitting data in various adsorption and kinetics models.

2. Experimental section

2.1. Materials and analytical methods

Acetic acid, copper sulfate, hydrochloric acid, nickel chloride, ammonia, and other reagents, of analytical grade, were purchased from the Shanghai Chemical Reagent Store (Shanghai, China), and used without further purification. Eggshells were collected from a local canteen of school.

2.2. Preparation of Amino-ESMs

Eggshell was rinsed with deionized water several times to remove the residual. ESM was obtained by immersing eggshell in a 40% acetic acid solution to dissolve the mineral shell. The obtained ESM was washed with deionized water several times to remove all the residuals, and then dried in an oven at 70˚C for 1 h. The dried ESM, 3 g, was added to a solution containing certain amount of ammonia (such as 13, 19, 27, 35, and 43 g) with 0.5 g of nickel chloride and reacted for 4 h under stirring. The fictionalizations of the ESM were performed according to Schemes 1 and 2. (Here, R refers to glycosaminoglycan and sialic acid carbon

$$\text{R-CHO} + \text{NH}_3 \xrightarrow{\text{Ni}^{2+}} \text{R-CH}_2\text{NH}_2 + \text{H}_2\text{O}$$

Scheme 1. Grafting of $-NH_2$ onto the surface of the ESM.

$$R_2C{=}O + NH_3 \xrightarrow{Ni^{2+}} R_2CHNH_2 + H_2O$$

Scheme 2. Grafting of $-NH_2$ onto the surface of the ESM.

ring structure associated with free aldehyde and keto groups on the surface of ESM.) After reaction, membrane was washed with deionized water to remove the excess reagent, and dried in an oven at 70°C for 1 h. The resulted membrane functionalized with 27 g of ammonia was designated as **Amino-ESM-27**.

2.3. Characterization of ESM and *Amino-ESM-27*

FT-IR spectra of the ESM, pristine, and Cu(II)-loaded **Amino-ESM-27** were scanned in the range of 400–4,000 cm/L with a collection of 16 scans on a Nicolet-740. The surface morphology of the pristine and Cu(II)-loaded **Amino-ESM-27** were also characterized using SEM (Hitachi S-4800), equipped with an energy dispersive X-ray (EDX) spectroscope, which was operated at EHT = 4.0 kV. Before SEM test, the **Amino-ESM-27** was coated with gold by a spatter coater to improve their conductivity for obtaining good quality of micrograph.

Water contact angle as well as the surface energy of the pristine and Cu(II)-loaded **Amino-ESM-27** were measured by the pendant drop method using a contact angle meter (SL200B, SOLON TECH, Shanghai, China), equipped with a CAST2.0 software, at 25 ± 1°C, under 70 ± 1% relative humidity condition. All reported values were the average of eight measurements taken at different locations of the same membrane surface.

2.4. Adsorption procedure

The required concentration of Cu(II) ions was prepared by dissolving certain amount of copper sulfate in deionized water. The desired solution pH was adjusted by adding either 0.1 mol/L NaOH or HCl solution. Adsorption experiments were carried out by exposing required dosage of adsorbent to a 250-mL solution in a 500-mL volumetric flask at desired temperature, using an automatic temperature-controlled water bath with an accuracy of ±1°C. The concentration of Cu(II) ions was analyzed by atomic absorption spectroscopy. The adsorption capacity of the adsorbent was evaluated using the following expression:

$$q = \frac{(C_0 - C_t)V}{m} \quad (1)$$

where q is the amount of Cu(II) ions adsorbed onto unit mass of the adsorbent (mg/g); C_0 and C_t represent the concentration of the Cu(II) ions in the initial solution and aqueous phase after adsorption for t minutes (mg/L); V is the volume of the aqueous phase (L); and m is the amount of adsorbent used (g), respectively.

2.5. Desorption of Cu(II) ions

Desorption of Cu(II) ions was performed using 0.1 mol/L HCl solution as a desorbing agent. The Cu (II)-loaded **Amino-ESM-27** sample was placed in a 150-mL desorption medium at 25°C, with a shaking speed of 150 rpm for 120 min. Then, the sample was washed with deionized water several times and subjected again to adsorption–desorption process for five cycles.

The percent of desorption was calculated using the following equation:

$$\%\ \text{Desorption} = \frac{m_1}{m_2} \times 100\,\% \quad (2)$$

where m_1 is the amount of Cu(II) ions desorbed (mg) and m_2 is the adsorbed amount of Cu(II) ions (mg) by adsorbent, respectively.

3. Results and discussion

3.1. Characterization of ESM

The FT-IR spectra of the ESM, pristine, and Cu(II)-loaded **Amino-ESM-27** are presented in Fig. 1. A strong and broad band appeared around 3,434.13 cm^{-1} is corresponded to O–H and N–H stretching vibrations. While the bands appearing at 1,641.15 and 1,546.65 cm^{-1} are attributed to the carbonyl group stretching and N–H bending, respectively. As for the spectrum of **Amino-ESM-27**, both of the bands attributed to N–H stretching and bending vibrations enhanced because of amino group grafting onto the surface of the ESM. Comparing the FT-IR spectra of the Cu(II)-loaded **Amino-ESM-27** with the pristine **Amino-ESM-27**, one can find that the intensity of the characteristic bands mentioned above of the former decreases slightly, which can be attributed to the interaction between O–H, N–H, and carbonyl groups of the **Amino-ESM-27** and Cu(II) ions.

Scanning electron microscopy has become an essential tool for characterizing the surface morphology and physical properties of a porous material. The surface morphologies of the pristine and Cu(II)-loaded

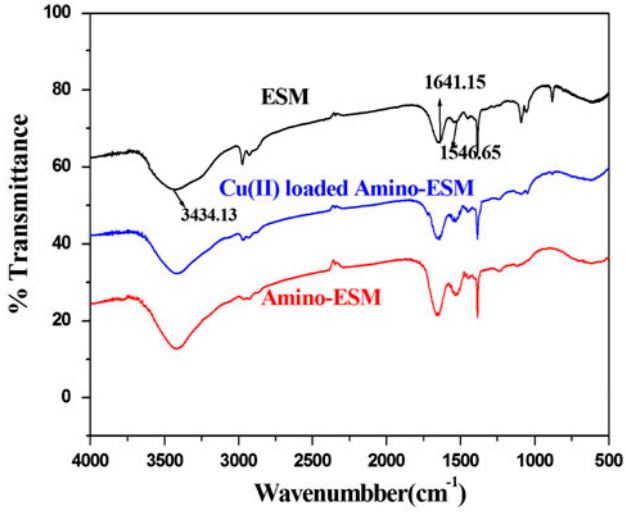

Fig. 1. FT-IR spectra of the ESM, pristine, and Cu(II)-loaded **Amino-ESM-27**.

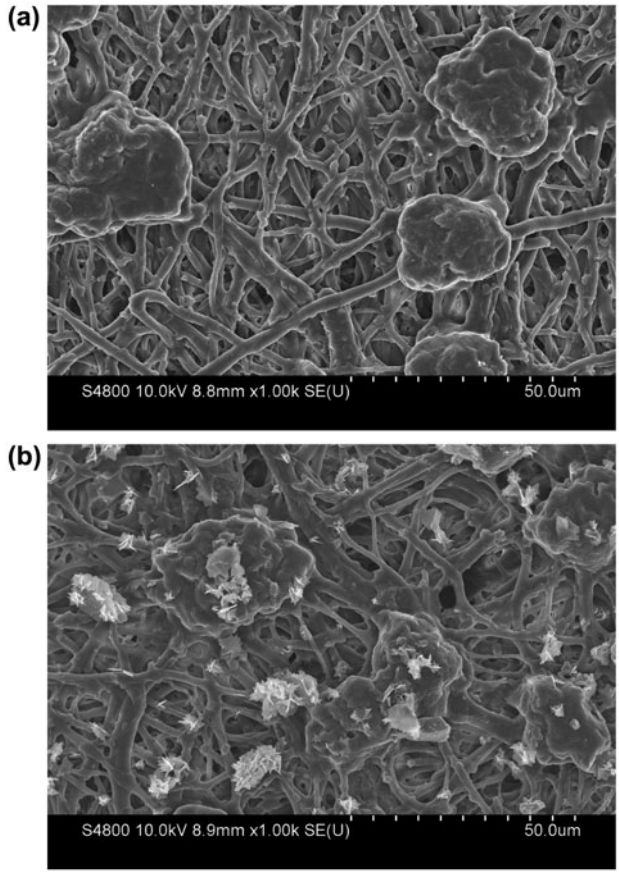

Fig. 2. SEM images of (a) pristine **Amino-ESM-27** and (b) Cu(II)-loaded **Amino-ESM-27**.

Amino-ESM-27 are shown in Fig. 2(a) and (b), respectively. A network-like structure with some prominences was observed on the pristine **Amino-ESM-27** surface (Fig. 2(a)), which indicated that the **Amino-ESM-27** consisted of highly cross-linked protein fibers and cavities. From Fig. 2(b), some plate-like white materials located on the **Amino-ESM-27** surface could be found clearly. This may be attributed to the aggregations of Cu(II) ions adsorbed on the **Amino-ESM-27** surface. Meanwhile, an EDX analysis was also carried out to further investigate the surface characteristic of pristine and Cu(II)-loaded **Amino-ESM-27**, and the results are shown in Fig. 3(a) and (b), respectively. From Fig. 3, the characteristic signal of Cu(II) could only be observed in Fig. 3(b).

Effects of the amount of ammonia used for grafting on the water contact angle and surface energy of the Amino-ESMs are presented in Fig. 4. It indicated that the water contact angle of the Amino-ESM decreased; however, the surface energy of the Amino-ESM increased quickly with an increase in amount of ammonia, until the amount of ammonia reached 27 g, then both of them kept nearly unchanged with a further increase in the amount of ammonia. This was attributed to more $–NH_2$ were grafted onto the surface of the ESM when more ammonia was used for reacting with ESM, which enhanced the hydrophilicity of the ESM. When amount of ammonia reached 27 g, almost all the active sites on the surface of the ESM were consumed; hence no more $–NH_2$ were grafted onto the surface of the ESM. The water contact angle and surface energy of the Cu(II)-loaded Amino-ESM are also showed in Fig. 4. It could be found that the adsorption of Cu(II) ions increased the water contact angle, however, decreased the surface energy of the Amino-ESM.

3.2. Investigation of important adsorption parameters

3.2.1. Effect of the amount of ammonia on adsorption

The adsorption performance of an adsorbent for heavy metal ions is greatly related to the functional groups on it. When ammonia reacts with the ESM using nickel chloride as catalysis, the $–NH_2$ groups are grafted on it. Due to strong chelating capacity of –N: with Cu(II), the adsorption capacity of Amino-ESM for Cu(II) is improved. To investigate the effect of the amount of ammonia on adsorption property, adsorption experiments were performed under the following conditions: adsorbent dosage of 0.4 g/L, solution pH 6.0, and initial Cu(II) ions concentration of 80 mg/L for 60 min. From Fig. 5, one found that the saturated adsorption amount of the Amino-ESM increased rapidly firstly, then kept almost unchanged

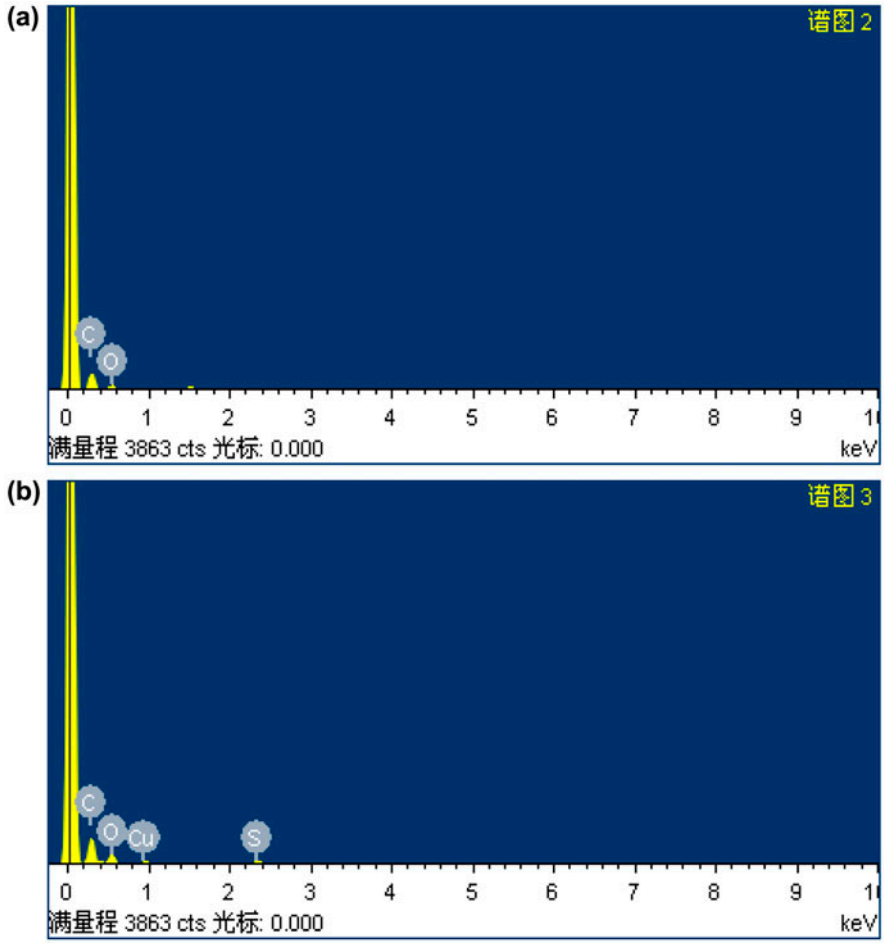

Fig. 3. EDX analysis of (a) pristine **Amino-ESM-27** and (b) Cu(II)-loaded **Amino-ESM-27**.

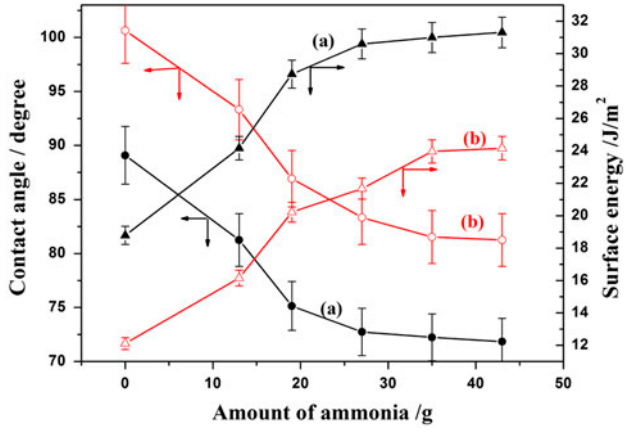

Fig. 4. Effects of the amount of ammonia used for grafting ESM on the water contact angle and surface energy of (a) pristine Amino-ESMs and (b) Cu(II)-loaded Amino-ESMs.

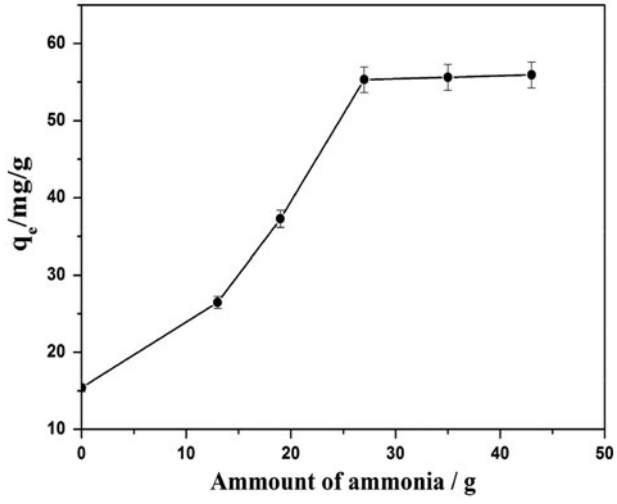

Fig. 5. Effect of the amount of ammonia on adsorption.

with further increase in the amount of ammonia. Introduction of more ligands (–NH_2) on the ESM surface at a higher ammonia amount increased the probable collision between the Cu(II) ions and the ligands leading to adsorption capacity enhancement. On the other hand, adsorption capacity was not elevated by further raise in ammonia amount from 27 to 43 g. As a result, it is concluded that the optimal ammonia amount for functioning ESM was 27 g. This result may be attributed to the limited active sites on the ESM surface for effective grafting of –NH_2. Therefore, the **Amino-ESM-27** was used for further adsorption investigations.

3.2.2. Effects of solution pH on adsorption

The solution pH has identified as one of the most important factors influencing the adsorption behavior due to its influence on the dissociation of active functional groups (such as –COOH and –NH_2) on the surface of **Amino-ESM-27** and different ionic forms of the copper in the solution. Meanwhile, H^+ are strongly competing with Cu(II) ions for the adsorption sites. Thus, the solution pH can affect greatly the adsorption capacity of **Amino-ESM-27** for Cu(II) ions. The adsorption experiment was carried out at solution pH in the range of 2.0–6.0, initial Cu(II) ions concentration of 80 mg/L, and adsorbent dosage of 0.4 g/L. Fig. 6(a) indicates that the adsorption capacity of **Amino-ESM-27** increases with an increase in solution pH. With an increase in solution pH, the competition between positively charged H^+ and Cu^{2+} for the same functional groups on the surface of **Amino-ESM-27** decreased. Meanwhile, as solution pH increases, the number of negatively charged groups on the surface of **Amino-ESM-27** also increased, which enhanced the adsorption capacity of **Amino-ESM-27**. As a result, a pH 6.0 was chosen for further adsorption experiment to avoid the precipitation of $Cu(OH)^{2+}$ as Cu(II) ions precipitate above pH 6.5 in the form of $Cu(OH)^{2+}$ [29].

To further understand the behavior of the solution during adsorption, the relationship between initial pH and adsorption equilibrium pH of solutions is presented Fig. 6(b). It indicated that the solution pH decreased during adsorption. As important functional groups on the surface of **Amino-ESM-27**, the H^+ dissociation ability of the –NH_2 groups is dependent on solution pH. Acidic surrounding inhibits the release of the H^+, while alkaline surrounding promotes the release of the H^+. As a result, with the increase in solution pH, more H^+ were released into the solution; hence, the ion exchange between Cu(II) ions and H^+ on the ion-exchange sites was also enhanced.

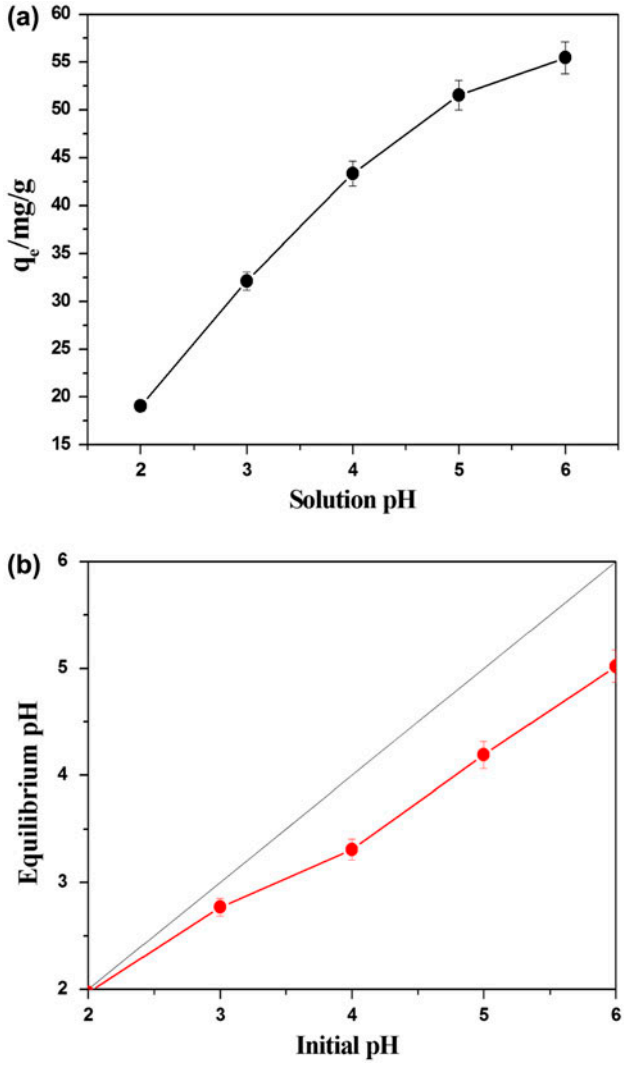

Fig. 6. (a) Effects of solution pH on adsorption and (b) relationship between equilibrium pH of solution and initial pH of solutions.

3.2.3. Effect of initial Cu(II) ions concentration on adsorption

In a batch adsorption process, the initial metal ions concentration of solution provides the necessary driving force to overcome the mass transfer resistance of metals between the solution and solid phases. Effect of initial Cu(II) ions concentration on adsorption behavior was studied at initial Cu(II) ions concentrations in the range of 20, 40, 60, 80, and 120 mg/L, solution pH 6.0, and adsorbent dosage of 0.4 g/L, and the results are presented in Fig. 7. It indicated that the uptake capacity of **Amino-ESM-27** increased from 14.94 to 70.17 mg/g. This was attributed to a higher initial Cu(II) ions concentration's increased driving

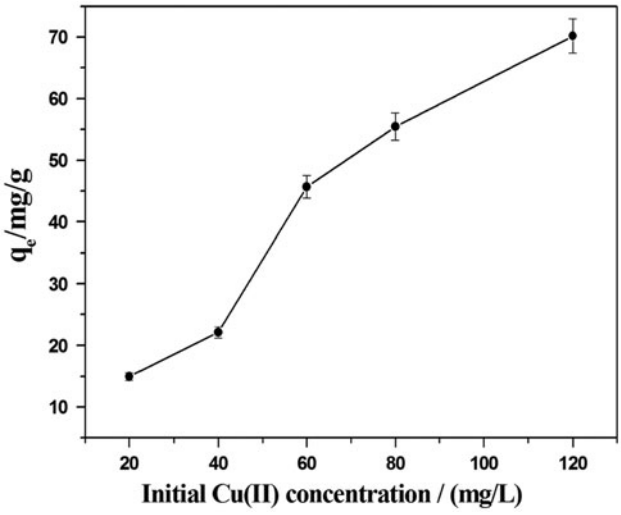

Fig. 7. Effect of initial Cu(II) ions concentration on adsorption.

force to overcome the mass transfer resistance of Cu (II) ions between the aqueous and solid phases, hence, resulted in a higher chance of chelating capacity between the Cu(II) ions and active functional groups on the surface of **Amino-ESM-27**.

3.2.4. Effect of adsorbent dosage on Cu(II) ions uptake by *Amino-ESM-27*

The adsorbent dosage is another important parameter because it has direct relation to the uptake capacity of an adsorbent under adsorption conditions. Effect of adsorbent dosage on adsorption behavior was studied at initial Cu(II) ions concentrations 80 mg/L, solution pH 6.0, and temperature of 25°C, and the result is shown in Fig. 8. The uptake capacity of **Amino-ESM-27** decreased rapidly from 86.3 to 55.1 mg/g, when the adsorbent dosage increased from 0.2 to 0.4 g/L. Then, uptake capacity of **Amino-ESM-27** decreased slowly with further increase in adsorbent dosage. Hence, based on efficient and economical point, adsorbent dosage of 0.4 g/L was used for further study.

3.2.5. Effect of ionic strength on adsorption

Generally, many different kinds of cations such as Na^+ and Ca^{2+} can be found in various industries wastewaters. The presence of ions leads to high ionic strength, which may significantly affect the behavior of the adsorption process. To investigate the effect of ionic strength on adsorption, the adsorption experiments were carried out using NaCl and $CaCl_2$ as the ionic medium in the range of 0–2.5 mmol/L. These tests were carried out at initial Cu(II) ions concentration of 80 mg/L, adsorbent dosage of 0.4 g/L for 60 min. Fig. 9 showed that when the concentration of both electrolytes increased from 0 to 2.5 mmol/L, the adsorption capacity of **Amino-ESM-27** decreased from 55.45 to 46.13 mg/g for Na-electrolyte and from 55.45 to 42.12 mg/g for Ca-electrolyte, respectively. This could be attributed to Na^+ and Ca^{2+} could compete with Cu(II) ions for the same adsorption sites on the surface of **Amino-ESM-27** and thus negatively affected the adsorption capacity of **Amino-ESM-27**. Meanwhile, the increase in the concentration of chloride anions in solution, which has a possibility of

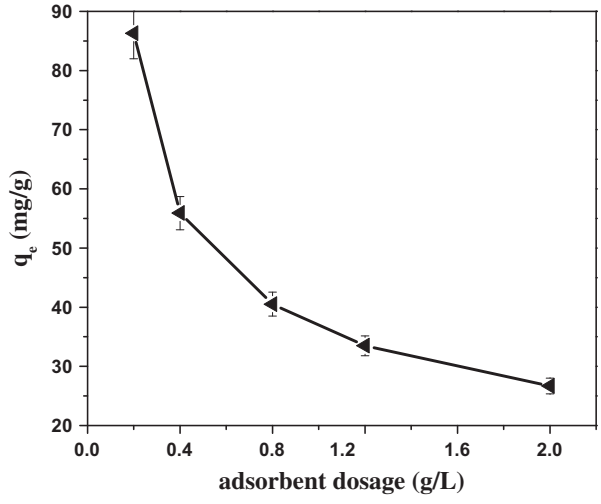

Fig. 8. Effect of adsorbent dosage on adsorption.

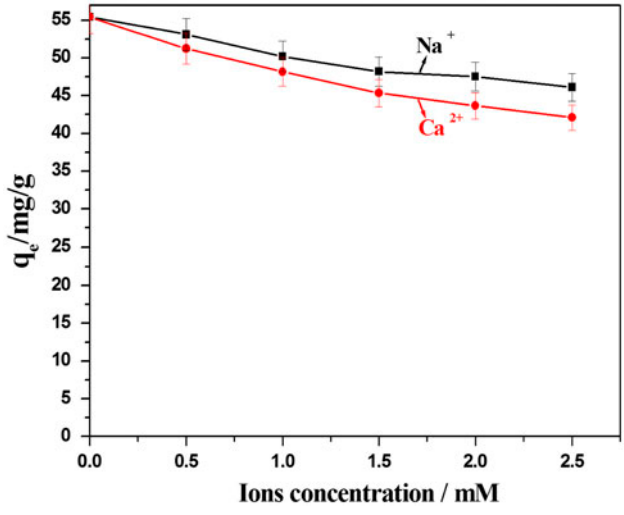

Fig. 9. Effect of ionic strength on adsorption.

the formation of uncharged species ($CuCl_2$) and negatively charged chloride complexes ($CuCl_3^-$ and $CuCl_4^{2-}$), also reduced the adsorption capacity of **Amino-ESM-27** [30]. The adverse effect of the ionic strength on Cu(II) ions uptake suggested the possibility of ion exchange being involved in the adsorption process.

3.2.6. Effects of temperature on adsorption

The effect of temperature on the adsorption capacity of the **Amino-ESM-27** was studied at 25, 30, 35, 40, 45, and 50°C, adsorbent dosage of 0.4 g/L, initial Cu (II) ions concentration of 80 mg/L, solution pH 6.0, and 60 min of contact time. The results presented in Fig. 10 demonstrate that the adsorption capacity increased slowly with an increase in temperature, which indicates the endothermic nature of the adsorption process in this study. The increase in Cu(II) uptake capacity with increasing temperature could be explained from two aspects: first, as the temperature rising, the diffusion of Cu(II) ions became much easier into the pore of **Amino-ESM-27** because of an increase in the degree of swelling of the adsorbent; secondly, bond rupture of the functional groups on the adsorbent surface at an elevated temperature increased the number of active adsorption sites, which also led to an enhancing adsorption capacity of the adsorbent.

3.2.7. Effect of contact time on adsorption

It is important to investigate the removal rate of heavy metal ions from aqueous solutions for the design and optimization of a wastewater treatment process. Effect of contact time on the adsorption capacity of **Amino-ESM-27** was carried out at solution pH 6.0 with an adsorbent dosage of 0.4 g/L and initial Cu(II) ions concentration in the range of 20, 40, 60, 80, and 120 mg/L. From Fig. 11, one observed that the adsorption capacity of **Amino-ESM-27** increased with an increase in contact time. Fig. 11 also indicated that the adsorption rate of **Amino-ESM-27** was rapid, and the adsorption equilibrium could be obtained within 60 min. Therefore, the adsorption experiments in the other parts were carried out for 60 min.

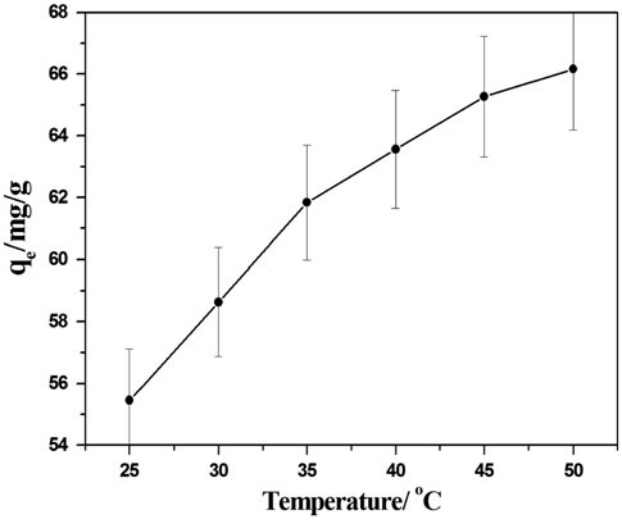

Fig. 10. Effects of temperature on adsorption.

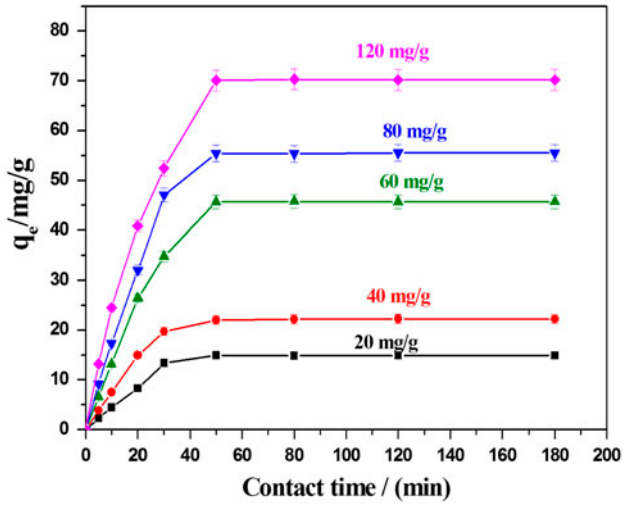

Fig. 11. Effects of contact time on adsorption.

3.3. Adsorption kinetics study

The knowledge of adsorption kinetics is important information for designing adsorption systems. To examine the adsorption kinetics of the **Amino-ESM-27**, four kinetic models, namely the non-linear form Lagergren pseudo-first-order and pseudo-second-order kinetic models [31], intraparticle diffusion model, and Crank model were examined and expressed as below [32]:

(1) non-linear form Lagergren pseudo-first-order kinetic model:

$$q_t = q_e(1 - \exp^{-k_1 t}) \tag{3}$$

(2) non-linear form Lagergren pseudo-second-order kinetic model:

$$q_t = \frac{k_2 q_e^2 t}{1 + k_2 q_e t} \tag{4}$$

(3) intraparticle diffusion model:

$$q_t = k_{\text{dif}}\ t^{1/2} \tag{5}$$

where q_e is the amount of adsorption at equilibrium, mg/g; q_t is the amount of adsorption at time t, mg/g; k_1 is the first-order rate constant, min^{-1}; k_2 is the second-order rate constants, min^{-1}; and k_{dif} is the intraparticle diffusion rate constant ($\text{mg/g min}^{-1/2}$).

The amount of adsorption equilibrium, q_e, the rate constants of the equation, k_1 and k_2, the calculated amount of adsorption equilibrium, $q_{e,c}$, and the coefficient of determination, R^2, calculated by non-linear method, are shown in Tables 1 and 2. The conformity between experimental data and the model predicted values was expressed by correlation coefficient (R^2). From Table 1 with Table 2, one observed that the pseudo-first-order equation fitted the experimental data better than that of the pseudo-second-order equation for its higher R^2. Meanwhile, the calculated amount of adsorption equilibrium ($q_{e,c}$) from the pseudo-first-order equation was close to the actual amount of adsorption equilibrium (q_e).

The relation plots of q_t vs. time $t^{1/2}$ are shown in Fig. 12. It showed the plot for each concentration of Cu(II) ions includes three stages: (I) the first stage corresponded to boundary layer diffusion or external surface adsorption, about 5 min; (II) the second stage was a gradual adsorption stage attributed to intraparticle diffusion, about 55 min; and (III) the final plateau region indicates equilibrium adsorption. The results indicated that the adsorption behavior of **Amino-ESM-27** was mainly controlled by the intraparticle diffusion.

(4) Crank model

The following two Crank diffusion models have usually been used to test the adsorption kinetics data for slab particle [33,34]:

$$\ln\left(\frac{C_t}{C_0}\right) = -k_f S_A t \tag{6}$$

$$\frac{q_t}{q_e} = 1 - \sum_{n=1}^{\infty} \frac{6}{\pi^2 n^2} \times \exp\left(\frac{-n^2\pi^2 D_S t}{r^2}\right) \tag{7}$$

where C_t is the bulk liquid-phase concentration, mg/L; C_s is the liquid-phase concentration at the surface in equilibrium with the solid-phase concentration, mg/L; k_f is the external mass transfer coefficient, m/s; S_A is the specific surface area of adsorbent, m^2/g; r is the half thickness of the adsorbent, m^{-1}; and D_S is the effective intraparticle diffusion coefficient of the adsorbent in the particle, m^2/s.

The dimensionless Biot number (B_i), which is the ratio of external transport to internal transport, is used for determination if the adsorption process is controlled by the mass transport of metal ions in the external boundary layer of the **Amino-ESM-27** or by the metal ions diffusion inside the pore of the **Amino-ESM-27**.

Table 1
The Lagergren pseudo-first-order rate constants calculated by non-linear method for Cu(II) ions adsorption onto the **Amino-ESM-27**

Metal ions	C_0 (mg/L)	q_e (mg/g)	k_1 ($\times 10^{-2}$ min^{-1})	$q_{e,c}$ (mg/g)	R^2
Cu(II)	20	14.94	4.58	15.43	0.9973
	40	22.14	5.22	24.17	0.9910
	60	45.71	6.81	45.06	0.9964
	80	55.45	8.07	54.24	0.9923
	120	70.17	8.35	77.35	0.9987

Table 2
The Lagergren pseudo-second-order rate constants calculated by non-linear method for Cu(II) ions adsorption onto the **Amino-ESM-27**

Metal ions	C_0 (mg/L)	q_e (mg/g)	k_2 ($\times 10^{-4}$ min^{-1})	$q_{e,c}$ (mg/g)	R^2
Cu(II)	20	14.94	4.12	21.92	0.8812
	40	22.14	4.07	42.78	00.9102
	60	45.71	3.88	98.27	0.9310
	80	55.45	2.21	105.98	00.9234
	120	70.17	1.98	113.21	0.9178

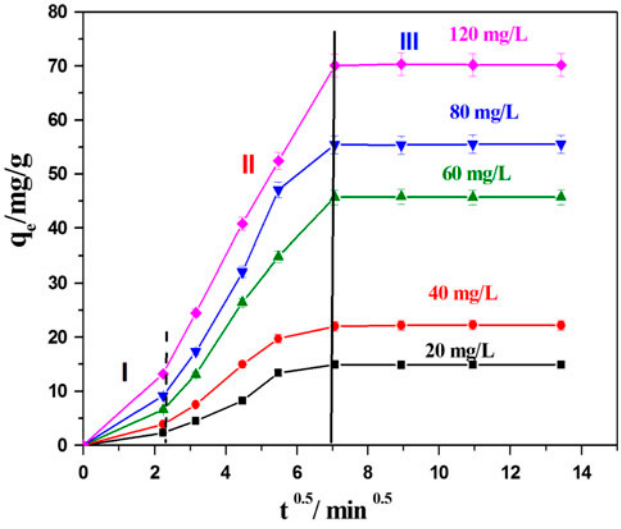

Fig. 12. Investigate intraparticular diffusion model for Cu(II) ions adsorption onto the **Amino-ESM-27**.

$$B_i = \frac{k_f r}{D_s} \tag{8}$$

When $B_i << 1$, it means that the external mass transfer is the controlling transport step. However, when $B_i >> 1$, it indicates that the metal ions diffusion through the pore of the porous adsorbent becomes the predominant mechanism. The B_i values calculated with experimental data are presented in Table 3. It was observed that all of B_i values were significant higher than one, which suggested that the adsorption process was mainly controlled by the intraparticle diffusion.

3.4. Adsorption isotherms study

Among the several isotherm models available, the Langmuir and Freundlich adsorption isotherms are the most frequently used ones. To understand and clarify the adsorption process, the non-linear form Langmuir adsorption isotherm and non-linear form Freundlich adsorption isotherm models were applied in this study.

The non-linear form Langmuir equation is [35]

$$q_e = \frac{q_{max} k_a C_e}{1 + k_a C_e} \tag{9}$$

where q_e is the amount adsorbed at equilibrium (mg/g), C_e is the equilibrium concentration (mg/L), q_{max} is the adsorption capacity (mg/g), and k_a is the adsorption intensity or Langmuir coefficient related to the affinity of the binding site (L/mg).

The non-linear form Freundlich equation is

$$q_e = K_F \, C_e^{1/n} \tag{10}$$

where K_F and $1/n$ are the constants that are related to the adsorption capacity and the adsorption intensity, respectively.

The isotherm constants were calculated by non-linear method and presented in Table 4. Taking into consideration, the values of the correlation coefficient (R^2) as a criterion for goodness of fit for the system, the Freundlich model showed better correlation ($R^2 = 0.9991$) than that of Langmuir model ($R^2 = 0.8684$), which indicated that Freundlich equation represented the adsorption process more ideally. From Table 4, one also could found that the value of

Table 3
Kinetic data from the Crank model and Biot number

Metal ions	C_0 (mg/L)	k_f ($\times 10^{-4}$m/s)	D_s ($\times 10^{-12}$m^2/s)	Biot
Cu(II)	20	1.52	1.32	218
	40	1.58	2.36	133
	60	2.17	3.49	118
	80	2.37	4.06	111
	120	2.41	4.28	106

Table 4
Kinetic data from the Langmuir isotherm and the Freundlich isotherm by non-linear method

Metals ion	Langmuir q_{max} (mg/g)	Isotherm k_a (L/mg)	Parameters R^2	Freundlich K_F (mg/g) (L/g)^n	Isotherm n	Parameters R^2
Cu(II)	214.574	0.062	0.8684	1.702	1.205	0.9991

n is 1.205, which indicated that the adsorption of **Amino-ESM-27** for Cu(II) ions was a favorable adsorption process.

3.5. Thermodynamic study

To investigate the mechanism involved in the adsorption, the thermodynamic behaviors of Cu(II) ion adsorption onto the surface of the **Amino-ESM-27** were evaluated employing the following equations:

$$K_d = \frac{C_0 - C_e}{C_e}\frac{V}{M} \tag{11}$$

$$\ln K_d = \frac{\Delta S^\circ}{R} - \frac{\Delta H^\circ}{RT} \tag{12}$$

$$\Delta G^\circ = -RT \ln K_d \tag{13}$$

where R is the ideal gas constant, 8.314 J K^{-1}/mol; T is the temperature in Kelvin; K_d is the distribution coefficient, L/g; C_0 is the initial concentration, mg/L; ΔH° is the enthalpy change; ΔS° is the entropy change; and ΔG° is the Gibbs free energy change in a given process, kJ/mol, respectively. The values of ΔH° and ΔS° can be calculated from the slope and intercept of the plot of ln K_d vs. $1/T$ presented in Fig. 13, respectively.

Thermodynamic parameters are calculated according to Eqs. (11)–(13) and illustrated in Table 5. The positive values of ΔH° confirmed the endothermic nature of the overall adsorption process. The positive value of ΔS° suggested the affinity of **Amino-ESM-27** toward Cu(II) ions. ΔG° values were negative, which indicated that adsorption was a spontaneous and favorable process. This value decreased with an increase in temperature indicating a better adsorption performance could be obtained with an increase in adsorption temperature.

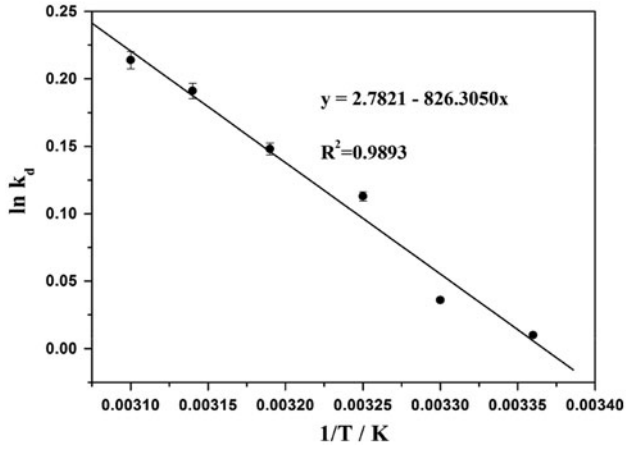

Fig. 13. Variation of ln K_d vs. $1/T$ for the adsorption of **Amino-ESM-27** for Cu(II) ions.

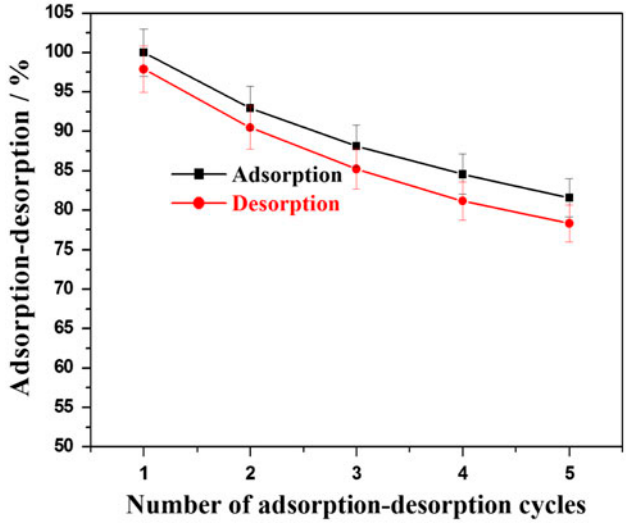

Fig. 14. Adsorption–desorption of the **Amino-ESM-27** for removing Cu(II) ions using 0.1 M HCl as the desorbing agent.

3.6. Regeneration of the *Amino-ESM-27*

The adsorption–desorption experiments were carried out to test the chemically stable and reusable adsorbent for the sake to qualify its practical use. Fig. 14 indicated that the adsorption capacity of **Amino-ESM-27** after five cycles only decreased 18.43%. This result implied that the prepared **Amino-ESM-27**

Table 5
Thermodynamic parameters calculated for the adsorption of Cu(II) ions onto the **Amino-ESM-27**

			−ΔG° (kJ/mol)					
Adsorbent	ΔH° (kJ/mol)	ΔS° (kJ/mol)	298.15 (k)	303.15 (k)	308.15 (k)	313.15 (k)	318.15 (k)	323.15 (k)
Amino-ESM-27	6.871	0.023	0.025	0.091	0.290	0.385	0.505	0.575

Table 6
Adsorption capacity of Cu(II) ions by various adsorbents

Adsorbent	Maximum adsorption capacity (mg/g)	References
Cu–PVA–SA	79.3	[2]
Hazelnut shell activated carbon (HSAC)	57.4	[3]
Lewatit TP-207	68.5	[4]
Hevea brasiliensis modified with sodium hydroxide	12.5	[5]
PGMA porous monolith	35.3	[9]
Chitosan/poly(vinyl amine) composite beads	158.1	[10]
Cashew nut shell	20.0	[11]
Polyaniline graft chitosan beads	25.3	[12]
Peanut hull	21.3	[36]
Cinnamomum camphora leaves powder	16.8	[37]
Litter of poplar forests	19.5	[38]
Lentil shell	9.0	[39]
Base-treated rubber leaves	15.0	[40]
Spent grain	10.5	[41]
Pretreated *Aspergillus niger*	2.6	[42]
Amino-ESM-27	70.2	Present work

could be used economically and effectively for treatment of wastewater containing Cu(II) ion at low concentrations.

3.7. Comparison of uptake capacity of *Amino-ESM-27* with other adsorbents

A comparison of the present maximum uptake capacity with the published results of various adsorbents is important to assess the potential application of the **Amino-ESM-27**. From Table 6, we found that the Cu(II) ions uptake capacity of the **Amino-ESM-27** in this work has large adsorption capacity.

4. Conclusion

In this study, amino groups were successfully grafted on the surface of the ESM and were used for adsorption removing Cu(II) ions from aqueous solution. FT-IR, SEM, EDX, and contact angle goniometer methods could be successfully used for investigating the different physicochemical properties of Amino-ESM before and after adsorption of Cu(II) ions. The batch adsorption experiment results indicated that grafting of amino group onto the ESM greatly enhanced the adsorption capacity of **Amino-ESM-27**, which was 2.5 times higher than that of the ESM. The adsorption rate of the **Amino-ESM-27** was fast and adsorption equilibrium was obtained within 60 min. Na^+ or Ca^{2+} coexists in the solution and only slightly decreased the adsorption capacity of **Amino-ESM-27**. Intraparticle diffusion model and Crank model indicated that intraparticle diffusion was the rate-controlling step. HCl could be used effectively for the regeneration of the **Amino-ESM-27**.

Acknowledgments

The authors would like to acknowledge the financial support of this work from National Natural Science Foundation of China (No. 21076174), Natural Science Foundation of Fujian (2014J01051). The authors also thank the anonymous referees for comments on this manuscript.

References

[1] Y. Ma, Q. Zhou, S.C. Zhou, W. Wang, J. Jin, J.W. Xie, A.M. Li, C.D. Shuang, A bifunctional adsorbent with high surface area and cation exchange property for synergistic removal of tetracycline and Cu^{2+}, Chem. Eng. J. 258 (2014) 26–33.
[2] J.H. Chen, H. Lin, Z.H. Luo, Y.S. He, Cu(II)-imprinted porous film adsorbent Cu–PVA–SA has high uptake capacity for removal of Cu(II) ions from aqueous solution, Desalination 277 (2011) 265–273.
[3] E. Demirbas, N. Dizge, M.T. Sulak, M. Kobya, Adsorption kinetics and equilibrium of copper from aqueous solutions using hazelnut shell activated carbon, Chem. Eng. J. 148 (2009) 480–487.
[4] M.H. Morcali, B. Zeytuncu, A. Baysal, S. Akman, O. Yucel, Adsorption of copper and zinc from sulfate media on a commercial sorbent, J. Environ. Chem. Eng. 2 (2014) 1655–1662.

[5] M.H. Kalavathy, L.R. Miranda, Comparison of copper adsorption from aqueous solution using modified and unmodified *Hevea brasiliensis* saw dust, Desalination 255 (2010) 165–174.
[6] C. Tizaoui, S.D. Rachmawati, N. Hilal, The removal of copper in water using manganese activated saturated and unsaturated sand filters, Chem. Eng. J. 209 (2012) 334–344.
[7] H. Duygu Ozsoy, H. Kumbur, B. Saha, J. Hans van Leeuwen, Use of *Rhizopus oligosporus* produced from food processing wastewater as a biosorbent for Cu(II) ions removal from the aqueous solutions, Bioresour. Technol. 99 (2008) 4943–4948.
[8] T.S. Anirudhan, P.S. Suchithra, Heavy metals uptake from aqueous solutions and industrial wastewaters by humic acid-immobilized polymer/bentonite composite: Kinetics and equilibrium modeling, Chem. Eng. J. 156 (2010) 146–156.
[9] J.X. Han, Z.J. Du, W. Zou, H.Q. Li, C. Zhang, Fabrication of interfacial functionalized porous polymer monolith andits adsorption properties of copper ions, J. Hazard. Mater. 276 (2014) 225–231.
[10] E.S. Dragan, A.I. Cocarta, M.V. Dinu, Facile fabrication of chitosan/poly(vinyl amine) composite beads with enhanced sorption of Cu^{2+}. Equilibrium, kinetics, and thermodynamics, Chem. Eng. J. 255 (2014) 659–669.
[11] P. SenthilKumar, S. Ramalingam, V. Sathyaselvabala, S. Dinesh Kirupha, S. Sivanesan, Removal of copper (II) ions from aqueous solution by adsorption using cashew nut shell, Desalination 266 (2011) 63–71.
[12] E. Igberase, P. Osifo, A. Ofomaja, The adsorption of copper (II) ions by polyaniline graft chitosan beads from aqueous solution: Equilibrium, kinetic and desorption studies, J. Environ. Chem. Eng. 2 (2014) 362–369.
[13] F.J. Alguacil, M. Alonso, F. Lopez, A. Lopez-Delgado, Uphill permeation of Cr(VI) using Hostarex A327 as ionophore by membrane-solvent extraction processing, Chemosphere 72 (2008) 684–689.
[14] K.Y. Wang, T.S. Chung, Fabrication of polybenzimidazole (PBI) nanofiltration hollow fiber membranes for removal of chromate, J. Membr. Sci. 281 (2006) 307–315.
[15] M.M. Nasef, A.H. Yahaya, Adsorption of some heavy metal ions from aqueous solutions on Nafion 117 membrane, Desalination 249 (2009) 677–681.
[16] Y.S. Chen, C.S. Chang, S.Y. Suen, Protein adsorption separation using glass fiber membranes modified with short-chain organosilicon derivatives, J. Membr. Sci. 305 (2007) 125–135.
[17] M.X. Loukidou, A.I. Zouboulis, T.D. Karapantsios, K.A. Matis, Equilibrium and kinetic modeling of chromium(VI) biosorption by *Aeromonas caviae*, Colloids Surf., A 242 (2004) 93–104.
[18] B. Preetha, T. Viruthagiri, Batch and continuous biosorption of chromium(VI) by *Rhizopus arrhizus*, Sep. Purif. Technol. 57 (2007) 126–133.
[19] W.T. Tsai, J.M. Yang, C.W. Lai, Y.H. Cheng, C.C. Lin, C.W. Yeh, Characterization and adsorption properties of eggshells and eggshell membrane, Bioresour. Technol. 97 (2006) 488–493.
[20] M. Arami, N.Y. Limaee, N.M. Mahmoodi, Investigation on the adsorption capability of egg shell membrane towards model textile dyes, Chemosphere 65 (2006) 1999–2008.
[21] S. Yoo, J.S. Hsieh, P. Zou, J. Kokoszka, Utilization of calcium carbonate particles from eggshell waste as coating pigments for ink-jet printing paper, Bioresour. Technol. 100 (2009) 6416–6421.
[22] F.G. Torres, O.P. Troncoso, F. Piaggio, A. Hijar, Structure–property relationships of a biopolymer network: The eggshell membrane, Acta Biomater. 6 (2010) 3687–3693.
[23] Z.K. Wei, C.L. Xu, B.X. Li, Application of waste eggshell as low-cost solid catalyst for biodiesel production, Bioresour. Technol. 100 (2009) 2883–2885.
[24] J.L. Tang, J. Li, J. Kang, L.W. Zhong, Y.H. Zhang, Preliminary studies of application of eggshell membrane as immobilization platform in sandwich immunoassay, Sens. Actuators, B 140 (2009) 200–205.
[25] G. Gergely, F. Wéber, I. Lukács, A.L. Tóth, Z.E. Horváth, J. Mihály, C. Balázsi, Preparation and characterization of hydroxyapatite from eggshell, Ceram. Int. 36 (2010) 803–806.
[26] Y.J. Zhang, W.D. Wang, L. Li, Y.M. Huang, J. Cao, Eggshell membrane-based solid-phase extraction combined with hydride generation atomic fluorescence spectrometry for trace arsenic(V) in environmental water samples, Talanta 80 (2010) 1907–1912.
[27] B. Zheng, L. Qian, H. Yuan, D. Xiao, X. Yang, M.C. Paau, M.M.F. Choi, Preparation of gold nanoparticles on eggshell membrane and their biosensing application, Talanta 82 (2010) 177–183.
[28] D. Mohan, C.U. Pittman Jr., Activated carbons and low cost adsorbents for remediation of tri- and hexavalent chromium from water, J. Hazard. Mater. 137 (2006) 762–811.
[29] K.G. Bhattacharyya, S.S. Gupta, Influence of acid activation on adsorption of Ni(II) and Cu(II) on kaolinite and montmorillonite: Kinetic and thermodynamic study, Chem. Eng. J. 136 (2008) 1–13.
[30] M. Safiur Rahmana, M. Rafiqul Islam, Effects of pH on isotherms modeling for Cu (II) ions adsorption using maple wood sawdust, Chem. Eng. J. 149 (2009) 273–280.
[31] K.V. Kumar, Linear and non-linear regression analysis for the sorption kinetics of methylene blue onto activated carbon, J. Hazard. Mater. B 137 (2006) 1538–1544.
[32] T.S. Anirudhan, P.G. Radhakrishnan, Chromium (III) removal from water and wastewater using a carboxylate-functionalized cation exchanger prepared from a lignocellulosic residue, J. Colloid Interface Sci. 316 (2007) 268–276.
[33] K.K.H. Choy, G. McKay, Sorption of cadmium, copper, and zinc ions onto bone char using Crank diffusion model, Chemosphere 60 (2005) 1141–1150.
[34] C.O. Illanes, N.A. Ochoa, J. Marchese, Kinetic sorption of Cr(VI) into solvent impregnated porous microspheres, Chem. Eng. J. 136 (2008) 92–98.
[35] K.V. Kumar, S. Sivanesan, Isotherm parameters for basic dyes onto activated carbon: Comparison of linear and non-linear method, J. Hazard. Mater. B129 (2006) 147–150.
[36] C.S. Zhu, L.P. Wang, W.B. Chen, Removal of Cu(II) from aqueous solution by agricultural by-product: Peanut hull, J. Hazard. Mater. 168 (2009) 739–746.
[37] H. Chen, G. Dai, J. Zhao, A. Zhong, J. Wu, H. Yan, Removal of copper(II) ions by a biosorbent—*Cinnamomum camphora* leaves powder, J. Hazard. Mater. 177 (2010) 228–236.

[38] M. Dundar, C. Nuhoglu, Y. Nuhoglu, Biosorption of Cu(II) ions onto the litter of natural trembling poplar forest, J. Hazard. Mater. 151 (2008) 86–95.
[39] H. Aydın, Y. Bulut, Çiğdem Yerlikaya, Removal of copper(II) from aqueous solution by adsorption onto low-cost adsorbents, J. Environ. Manage. 87 (2008) 37–45.
[40] W.S.W. Ngah, M.A.K.M. Hanafiah, Biosorption of copper ions from dilute aqueous solutions on base treatedrubber (*Hevea brasiliensis*) leaves powder: kinetics, isotherm, and biosorption mechanisms, J. Environ. Sci. 20 (2008) 1168–1176.
[41] S. Lu, S.W. Gibb, Copper removal from wastewater using spent-grain as biosorbent, Bioresour. Technol. 99 (2008) 1509–1517.
[42] M. Mukhopadhyay, S.B. Noronha, G.K. Suraiskhumar, Kinetic modelling for the biosorption of copper by pretreated *Aspergillus niger* biomass, Bioresour. Technol. 98 (2007) 1787–1787.